Journal of Hydrology 409 (2011) 512–524

Contents lists available at SciVerse ScienceDirect

Journal of Hydrology

journal homepage: www.elsevier.com/locate/jhydrol

Evaluating the effects of parameterized cross section shapes and simplified routing with a coupled distributed hydrologic and hydraulic model

A.I. Mejia *, S.M. Reed

NOAA, NWS, Office of Hydrologic Development, Silver Spring, MD, USA

ARTICLE INFO

Article history:
Received 19 December 2010
Received in revised form 22 April 2011
Accepted 25 August 2011
Available online 1 September 2011
This manuscript was handled by Konstantine P. Georgakakos, Editor-in-Chief, with the assistance of Vincent S. Neary, Associate Editor

Keywords:
Distributed model
Routing
Cross section geometry

SUMMARY

With spatially distributed hydrologic models the need arises for determining the channel cross section shape for the entire stream network. In the absence of cross section data, assumed or parameterized cross section shapes are often used. The effects of parameterized cross sections are evaluated in this study by developing a modeling framework that externally couples a spatially distributed hydrologic model, HL-RDHM, with a one-dimensional unsteady hydraulic model, HEC-RAS. The evaluation emphasizes the effects of parameterized cross sections on simulated flows by focusing the analysis on the portion of the basin's main stream reach where detailed cross section data and observed streamflows (at both ends of the reach) are available, and by developing and testing three cross section scenarios. The scenarios are designed to increase sequentially, in a stepwise fashion, the complexity of the parameterized cross section, starting with a single roughness parameter and channel power law cross section shape and then including additional power law or roughness parameters. This is done stepwise to help distinguish the effects associated with each parameterization, and decide the required level of cross section detail. The scenario simulations are evaluated using split sampling, changes in measures of performance and hydrograph agreement, hypothesis tests on Nash–Sutcliffe values, and overall predictive uncertainty. The coupling framework is applied to the Blue and Illinois River basins, in Oklahoma, US. Overall, we found that in these basins the coupling tends to improve predictions when dynamic wave routing and floodplain cross section geometry are considered concurrently. For this scenario, we found that on average typical measures of model performance may be improved and, based on a quantitative and qualitative assessment, uncertainty may be reduced. We also found that dynamic wave routing does not tend to perform better than kinematic wave routing for the most basic scenarios with a single power law cross section shape. Further, results indicate that the distributed hydrologic model performance at the main outlet and at the upstream boundary of the hydraulic model, and the relative contribution of lateral inflows, are key factors that need to be considered when deciding the applicability of the coupled framework to other basins. In the future, to effectively use resources, it will be beneficial to automate the coupling and accompany its application with a priori criteria for selecting those basins where benefits are most likely.

1. Introduction

In an effort to understand and improve distributed hydrologic models, the Office of Hydrologic Development (OHD) of the National Oceanic and Atmospheric Administration's National Weather Service (NOAA/NWS) led the Distributed Model Intercomparison Project (DMIP 1) and is currently leading a second phase (DMIP 2) (Reed et al., 2004; Smith et al., 2004b, 2009). Some goals of DMIP include determining the level of model complexity needed to achieve improved predictions while keeping the parameterization costs low and identify areas in the overall modeling process to focus improvement efforts. The experience with DMIP 1 and 2 has highlighted some of the complications that can arise when trying to compare and evaluate hydrologic models (Butts et al., 2004; Reed et al., 2004; Smith et al., 2009). Factors such as high dimensionality, uncertainty (i.e. input, structural, parametric, and output), and limited data availability for model evaluation, make the identification of specific causes of model deficiency difficult (Reed et al., 2004). This suggests the need for more targeted model assessments and comparisons, where a distinct component of the model is evaluated (Reed et al., 2004). In this study we follow this suggestion through a more detailed examination of the routing technique and parameterization used in the Hydrology Laboratory Research Distributed Hydrologic Model (HL-RDHM). HL-RDHM is a distributed hydrologic model developed for forecasting purposes (Koren et al., 2003, 2004). The kinematic wave routing technique implemented in HL-RDHM is common to several other distributed

* Corresponding author. Address: Office of Hydrologic Development, W/OHD, National Weather Service, 1325 East-West Highway, Silver Spring, MD 20910, USA. Tel.: +1 301 713 0640x149; fax: +1 301 713 0963.

E-mail address: alfonso.mejia@noaa.gov (A.I. Mejia).

0022-1694/$ - see front matter © 2011 Elsevier B.V. All rights reserved.
doi:10.1016/j.jhydrol.2011.08.050

hydrologic models (e.g. see Table 1 in Reed et al., 2004). Therefore, the conclusions from our analysis here are relevant to other models as well.

With this in mind, and noting that the routing process plays an important role in hydrologic forecasting (Fread, 1981, 1993; Moreda et al., 2009), we are interested in examining ways in which the routing process may be improved. Many times there is concern that a simpler routing conceptualization may cause substantial loss of predictive capability (Horritt and Bates, 2002; Romanowicz and Beven, 2003; Cook and Merwade, 2009; Moreda et al., 2009). Further, there are aspects of the routing process that have received little attention but have, concurrently, gained a more prominent role within a spatially distributed context (Orlandini and Rosso, 1996, 1998; Koren et al., 2004). A good example of the latter is the role played by the cross section geometry in the routing of flows (Orlandini and Rosso, 1996, 1998; Koren et al., 2004). Cross section data is generally lacking but still required in a distributed context, the de facto alternative has been to use parameterized cross section shapes (e.g. Fread and Lewis, 1986; Orlandini and Rosso, 1996, 1998; Koren et al., 2004; Valiani and Caleffi, 2009), and many times a simple analytical shape is assumed. However, the effects of parameterized cross section shapes on simulated flows have been studied little and indications are that they can have an influential effect. For example, Orlandini and Rosso (1998), in a relatively recent study, showed that parameterized cross sections with vertically varying widths based on relationships of hydraulic geometry, as opposed to rectangular shapes with constant width, can lead to considerable improvement in flow simulations using a distributed model. Other studies have examined directly the role of cross section shapes but not for distributed hydrologic modeling (e.g. Keefer, 1976; Garbrecht, 1990; Myers, 1991; Ponce and Porras, 1995).

With this background, the aim of this study is to examine the effects that parameterized cross section shapes and simplified routing (i.e. kinematic wave routing instead of more general dynamic routing) have on simulated flows within the context of distributed hydrologic modeling. This study's motivation stems from the perception that using an approximate cross section shape may have a sufficient influence on routed flows to reduce gains from a more general routing method (Keefer, 1976; Myers, 1991; Ponce and Porras, 1995; Orlandini and Rosso, 1998). We seek to test this hypothesis by performing various model-based experiments while trying to emphasize conditions relevant to the use of hydrologic and hydraulic models in NWS forecasting operations.

2. Background

Much of the stage and background for this investigation is set by the results and data sets from DMIP 1 and 2 (Reed et al., 2004; Smith et al., 2004b, 2009). We use the data available to DMIP 1 participants and one of the participating models, HL-RDHM (Koren et al., 2004; Smith et al., 2004b). Next, the study area and data sets used are briefly described (see Smith et al. (2004b) for details).

2.1. Study area

The basins selected for this study are located on the Blue and Illinois River (Fig. 1a shows their location). Hereafter these basins are simply referred to as the Blue or Illinois River. Both basins are part of DMIP 1 and 2 (Smith et al., 2004b, 2009). This has the advantage that for these basins the quality of required data sets (i.e. input forcings and streamflow observations) has been thoroughly inspected and the performance of HL-RDHM has been tested beforehand (Koren et al., 2004; Reed et al., 2004; Smith et al., 2004b; Zhang et al., 2004). With this, we can draw attention to the modeling of the routing process and place less emphasis on other aspects of distributed modeling.

The Blue River basin, located in Oklahoma (see Fig. 1a), has an overall drainage area of approximately 1233 km^2. The Illinois River basin, located between the Oklahoma–Arkansas border (see Fig. 1a), has a drainage area of approximately 2484 km^2. We use two streamflow gauges for each basin, an outlet gauge located at the overall basin outlet and an interior gauge located further upstream from the outlet gauge (see Fig. 1b and c for the location of the gauges in the Blue and Illinois River basins, respectively). In the Blue River, the outlet gauge is near Blue (United States Geological Survey (USGS) gauge number 07332500), and the interior upstream gauge is near Connerville (USGS gauge number 07332390). In the Illinois River, the gauge near Tahlequah is the outlet gauge (USGS gauge number 07196500) while the interior gauge is near Watts (USGS gauge number 07195500). The along-stream distance between the two gauges in the Blue River is approximately 84.5 km. The distance is shorter in the Illinois River, approximately 71.2 km. However, the Blue River has more tributary streams (i.e. inflow locations) connecting to the main stream reach. Hereafter, for clarity, the river section between the internal and outlet gauge is referred to as the main stream reach. The stream network connectivity is shown in Fig. 1b and c for the Blue and Illinois River, respectively. The 4 km grid cell sizes in this

Table 1
Summary of the average values of NS, R_{mod}, $|\Delta Q_p|/Q_{p,obs}$, and $|\Delta T_p|/T_{p,obs}$ for the baseline simulations (KW and DW4) and the three cross section parameterization scenarios (DW1, DW2, and DW3), in both the Blue and Illinois River basins. The results for the hypothesis tests defined in (8) and (9) are also shown. For the hypothesis tests, the numbers associated with each simulation are the number of individual storm events that agree with the alternative hypothesis where the total number of events is 11 and 23 for Blue and Illinois, respectively.

Basin	Simulation	Calibration		Validation		$\lvert\Delta Q_p\rvert/Q_{p,obs}$	$\lvert\Delta T_p\rvert/T_{p,obs}$	Hypothesis test	
		NS	R_{mod}	NS	R_{mod}			Test in (8)[a]	Test in (9)[b]
Blue River	KW	0.75	0.78	0.67	0.69	0.30	0.16	–	6
	DW1	0.7	0.73	0.7	0.69	0.32	0.15	4	3
	DW2	0.71	0.73	0.74	0.7	0.30	0.17	5	2
	DW3	0.68	0.74	0.7	0.69	0.30	0.19	5	3
	DW4	0.74	0.79	0.7	0.7	0.30	0.14	6	–
Illinois River	KW	0.91	0.88	0.81	0.85	0.10	0.066	–	17
	DW1	0.95	0.93	0.84	0.83	0.14	0.081	9	13
	DW2	0.95	0.93	0.85	0.83	0.14	0.078	9	13
	DW3	0.97	0.98	0.85	0.87	0.09	0.052	17	10
	DW4	0.97	0.98	0.84	0.86	0.11	0.028	17	–

[b] Number of individual storm events i that agree with Ha: $NS_i < NS_{i,DW4}$.
[a] Number of individual storm events i that agree with Ha: $NS_i > NS_{i,KW}$.

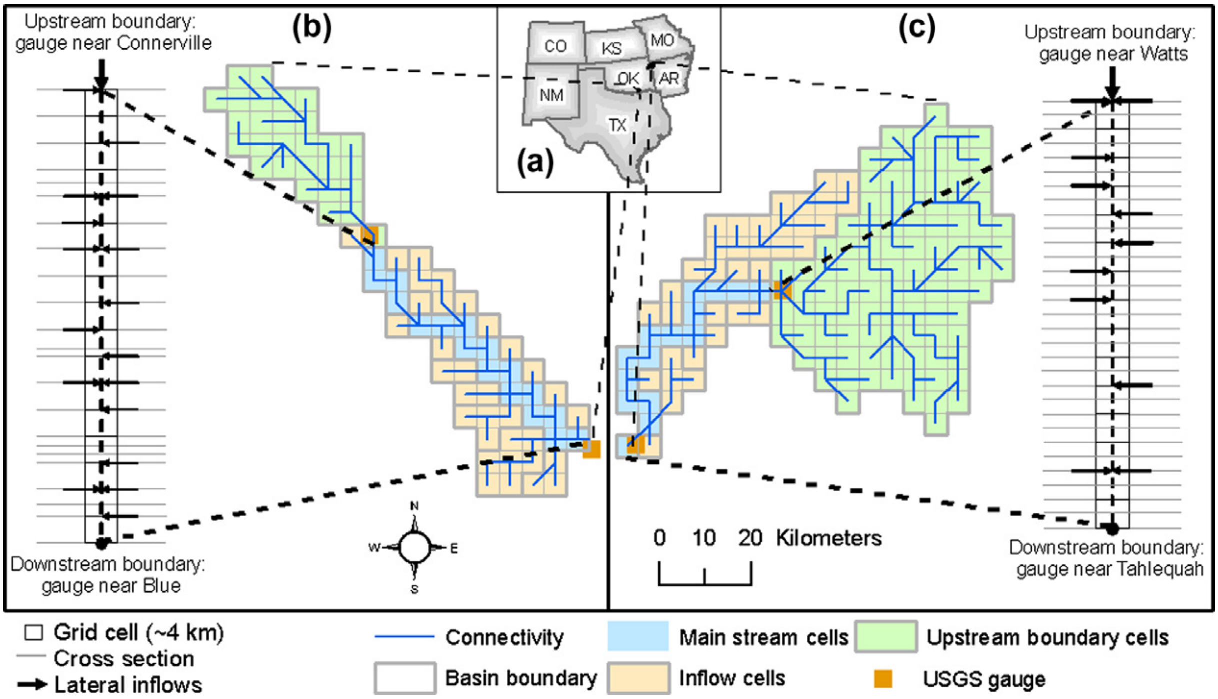

Fig. 1. (a) Map illustrating the location of the Blue and Illinois River basins. Illustration of the basin boundary, stream network connectivity, location of streamflow gauges, cell classification used in coupling, and routing reach for the (b) Blue and (c) Illinois River basins.

application match the nominal size of the radar-based precipitation products used in the modeling. This 4 km grid stream network connectivity was derived from 30-m digital elevation model (DEM) data following the method developed by Reed (2003) for NWS applications.

The contributing drainage area between the two gauges in each basin is approximately the same, 813 km^2 for the Blue River and 839 km^2 for the Illinois River. Nevertheless, relative to the overall drainage area, the area contributing to lateral inflows along the main stream reach is approximately 66% in the Blue River and 34% in the Illinois River. Thus, lateral inflows are expected to play a larger role in the Blue River. The soil types in the Blue River are comprised of clay, loam, sandy clay, and clay loam. In the Illinois River the soil types are silty clay, silty clay loam, and silt loam. Most of the land use in the Illinois River is pasture and forest, while Blue is mostly agricultural. The mean annual rainfall and runoff coefficient are approximately 1036 mm and 0.17, respectively, for the Blue River, and 1157 mm and 0.26, respectively for the Illinois River (Smith et al., 2004b). Additionally, Smith et al. (2004a) noted that conditions in the Blue River, in contrast with other basins in the same hydroclimatic region, are such that little basin response filtering tends to occur and rainfall spatial variability is higher.

2.2. Data sets

We used mainly data sets available for DMIP 1 and 2 (the data sets can be found at http://www.nws.noaa.gov/oh/hrl/hsmb/hydrology/index.html). Smith et al. (2004b) describe these data sets in detail. Here we only describe the data sets that were not part of DMIP 1 and 2, either because they were unavailable at the time or not used.

For the interior gauge in the Blue River at Connerville, we obtained streamflow data from the USGS at the 1 h resolution for the period between October 1, 2003, and December 31, 2007. The detailed cross section data for the Blue River was derived from field surveys, bridge plans, and pier scour studies (Smith et al., 2004b). Additionally, we linearly interpolated cross sections in the Blue River based on the interpolation method in HEC-RAS (Brunner, 2008b) so that at least one detailed cross section fell within every grid cell on the main stream reach. The grid cell structure for the Blue and Illinois River is shown in Fig. 1b and c, respectively. For the Illinois River, the cross section data were derived from USGS topographic maps at 1″ = 2000′ resolution (Smith et al., 2004b). From the available data, the cross section spacing for the Blue River is on average 3 km and for the Illinois River is approximately 2 km. The cross section locations for the Blue and Illinois are illustrated in Fig. 1b and c, respectively, in a schematic diagram of the main stream reach.

3. Modeling framework

To carry out the proposed experiments, we externally coupled a distributed hydrologic model, HL-RDHM, with a more general hydraulic routing model, the Hydrologic Engineering Center's River Analysis System, HEC-RAS (Brunner, 2008a,b). The way this coupling is done and the calibration strategy employed are described below.

We chose HEC-RAS because it is readily available and it numerically solves the complete 1-dimensional, shallow wave/St. Venant equations (Brunner, 2008a,b), providing a more general routing method than HL-RDHM. HL-RDHM solves numerically the kinematic wave approximation to the shallow wave/St. Venant equations (Koren et al., 2004). Both HL-RDHM and HEC-RAS employ a similar weighted four-point implicit finite difference approximation in their numerical solution (Koren et al., 2004; Brunner, 2008a).

3.1. Coupling of HL-RDHM and HEC-RAS

For the coupling, the HL-RDHM grid representation of a basin is classified into the following three types of grid cells: main channel, contributing lateral inflow, and contributing upstream boundary cells. Fig. 1b and c illustrates this cell classification scheme for the Blue and Illinois River, respectively. The main channel cells are the grid cells that comprise the main stream in the connectivity network. In the connectivity network the main stream is identified as the cells having the largest drainage area when moving upstream from the overall basin outlet. The contributing lateral inflow cells consist of the sub-basins draining to the main channel cells. The contributing upstream boundary cells are the sub-basin cells draining to the most upstream boundary of the hydraulic model.

The coupling between HL-RDHM and HEC-RAS is directional and external, similar to the approach of Lian et al. (2007) which proved to be successful at improving predictions but using a different, semi-distributed, hydrologic model. The directionality comes from neglecting potential feedbacks between the two models such as backwater effects on tributaries and hyporheic exchanges along the main stream. The coupling is external because the continuous output from HL-RDHM is used as continuous input, i.e. lateral inflow, into HEC-RAS, while the two models remain independent from each other. The lateral inflow cells for the Blue and Illinois River are shown in Fig. 1b and c, respectively. Because of the relatively large size of each grid cell (approximately 16 km^2), the contributions from surface and subsurface hillslope runoff within each main channel cell are added to their associated inflow locations. The main channel cells for Blue and Illinois are shown in Fig. 1b and c, respectively. We preserve initially in HEC-RAS the channel and cross section parameters used for routing in HL-RDHM, such as the channel length, the roughness parameter, and the power law cross section parameters (Koren et al., 2004). However, the roughness and power law parameters are varied hereafter (in Section 5) to quantify their effects on flows.

The coupled model routes the exact same flows as HL-RDHM along the portion of the main stream shared by both models. For the simplest comparison, when parametric cross-section geometry from HL-RDHM is also used to build cross-sections in HEC-RAS, the only major difference between the two models is the kinematic versus dynamic wave solution.

3.2. Baseline simulation for HL-RDHM and the coupled model

HL-RDHM and the coupled HEC-RAS model with detailed cross section data are both treated as baseline simulations and used for comparisons in Sections 5 and 6. Hereafter, the baseline HL-RDHM simulation is referred to as distributed hydrologic kinematic wave simulation (KW), while the coupled HEC-RAS baseline simulation is referred to as distributed hydrologic dynamic wave simulation four (DW4). The number four after DW is used to distinguish the coupled baseline simulation from other coupled simulations described hereafter. DW4 has the distinctive characteristic that it uses detailed cross section data to route flows. DW4 is treated as a baseline simulation because it represents the most general and detailed model structure implemented in this study. DW4 serves as a potential upper limit when assessing predictive gains from different cross section scenarios. On the opposite end, KW is considered a baseline simulation because it represents the simplest model structure used and serves as a potential lower limit.

3.3. Calibration of baseline simulations

HL-RDHM and HEC-RAS were calibrated separately based on different objectives. Two HL-RDHM kinematic wave routing parameters that influence the timing and the shape of hydrographs were adjusted with constant multipliers across all model cells to improve the overall fit of simulated and observed streamflows at the main outlet. HEC-RAS accepted the calibrated inflows from HL-RDHM at the model interface cells and HEC-RAS Gauckler–Manning's roughness coefficients in the main channel were calibrated to provide the best match with observed flow at the basin outlet. Ultimately the coupled model is used to test several scenarios but only with data from the validation period. The data used in the calibration of HL-RDHM and HEC-RAS are not considered in the analysis of results.

The data periods used for the calibration and validation of HL-RHDM and HEC-RAS are summarized in Fig. 2. To warm-up HL-RDHM, we used the first year prior to the start of the calibration period for the Blue River and the 6 months prior for the Illinois River. To initialize HEC-RAS, a backwater steady state approach together with the observed flow at the start of the calibration period was used (Brunner, 2008b). In the HEC-RAS model, the downstream boundary was moved further downstream to minimize the effects from assuming normal flow as the downstream boundary condition (Singh et al., 1997). To calibrate HL-RDHM the automatic method of Kuzmin et al. (2008) was used together with parameter information from previous modeling studies (Reed et al., 2004). HEC-RAS was calibrated manually by adjusting the local channel Gauckler–Manning's roughness parameters. To adjust the Gauckler–Manning's roughness parameters for HEC-RAS, the same scaling factor approach used for distributed hydrologic parameters was implemented (Koren et al., 2004).

The calibration performance of DW4 was assessed from the values of the Nash–Sutcliffe (NS) and modified correlation (R_{mod}) coefficient (Nash and Sutcliffe, 1970; McCuen and Snyder, 1975), and from visual evaluation. The NS and R_{mod} values found for the calibration and validation of KW and DW4 are summarized in Table 1.

4. Parameterization of cross section shapes

Various parameterizations have been proposed to represent the cross section shape (Henderson, 1966; Fread and Lewis, 1986; Garbrecht, 1990; Knight, 2006; Valiani and Caleffi, 2009). The power law cross section shape remains popular in hydrologic modeling because it has been shown to be applicable to a range of conditions and requires few parameters (Henderson, 1966; Fread and Lewis, 1986; Garbrecht, 1990; Orlandini and Rosso, 1996, 1998; Koren et al., 2004). The power law relationship is as follows:

$$\frac{B}{B_r} = \left(\frac{H}{H_r}\right)^b, \tag{1}$$

where B [L] is the channel top width, B_r [L] is a reference width, H [L] is the channel depth, H_r [L] is a reference depth, and the exponent b controls the shape of the cross section. The cross section shape is rectangular for $b = 0$, parabolic for $b = 0.5$, triangular for $b = 1$, and an expanding shape for $b > 1$ where the width of the section increases non-linearly with depth. By letting $a = B_r H_r^{-b}$, the relationship in (1) can be written as:

$$B = aH^b. \tag{2}$$

Integrating (2) over the interval 0 to H, and substituting back into (2), results in:

$$B = [a(b+1)^b]^{1/(b+1)} A^{b/(b+1)}. \tag{3}$$

A [L^2] is the cross section area. To estimate a priori values of the channel shape parameters a and b, the power law can be related to the Gauckler–Manning equation as follows:

$$Q = \frac{\sqrt{S}}{n}\left[a(b+1)^b\right]^{-2/3(b+1)} A^{(b+5/3)/(b+1)}, \tag{4}$$

where S is the local channel slope and n is the channel roughness parameter. The relationship (4) can also be written as:

$$Q = Q_s A^m, \tag{5}$$

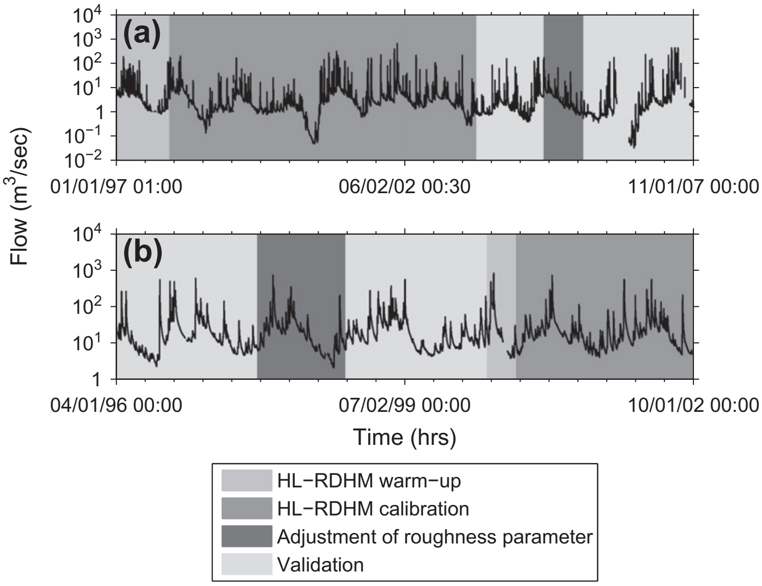

Fig. 2. Complete calibration and validation periods for the (a) Blue and (b) Illinois River basins. The complete period for the Blue River is 01/01/1997–10/31/2007 and for the Illinois River is 04/01/1996–09/30/2002. To calibrate HL-RDHM routing parameters the period from 01/01/1998 to 10/01/2003 and from 10/01/2000 to 10/01/2002 were chosen for the Blue and Illinois River, respectively. To adjust the roughness parameter in the coupled model, the period from 01/01/2005 to 10/05/2005 and from 11/01/1997 to 10/30/1998 were chosen for the Blue and Illinois River, respectively. The above periods were chosen to increase the overlap between observed flows at the outlet and interior gauge during the validation period.

where

$$Q_s = \frac{\sqrt{S}}{n}\left[a(b+1)^b\right]^{-2/3(b+1)}, \text{ and} \qquad (6)$$
$$m = (b + 5/3)/(b + 1).$$

Using (5) to express Eq. (4) is useful because it shows that a priori cross section shape parameters can be estimated from flow and cross sectional area measurement data when available. These data are commonly measured by the US Geological Survey when building flow-stage rating curves for stream gauging stations. The previous relationships are applicable at a given channel section, assuming the channel to be prismatic along this section. To estimate a priori cross section parameters for other channel sections in the basin's stream network, a methodology based on basin geomorphology is developed in Koren et al. (2004).

A second power law cross section, similar to (2), may be used to account for the floodplain shape as follows (Fread and Lewis, 1986; Garbrecht, 1990; Singh, 1996):

$$B = c(H - H_b)^d + B_b, \qquad (7)$$

where c and d have the same meaning as a and b in (2), respectively, but are only for the floodplain. H_b is the channel bankfull depth and B_b is the channel width at H_b. (2) is used for $H \leqslant H_b$ and (7) when $H > H_b$. The relationships (1)–(7) are used to estimate parameterized cross section shapes.

5. Application of the modeling framework

5.1. Simulation scenarios

Three scenarios are proposed. The scenarios are chosen keeping in mind their applicability in a distributed hydrologic modeling context. The scenarios are designed to successively increase, in a stepwise fashion, the complexity of the parameterized cross sections by incorporating additional cross section power law or roughness parameters. The succession of cross section detail is illustrated in Fig. 3. The local stepwise approach to model structural evaluation taken for this study is appropriate because we are only focusing on the routing process. Nevertheless, there are generalized methods available to explore and identify model structural deficiencies globally (Lin and Beck, 2007; Reichert and Mieleitner, 2009). These methods will be more appropriate when the entire model structure is being examined and the coupling is not external.

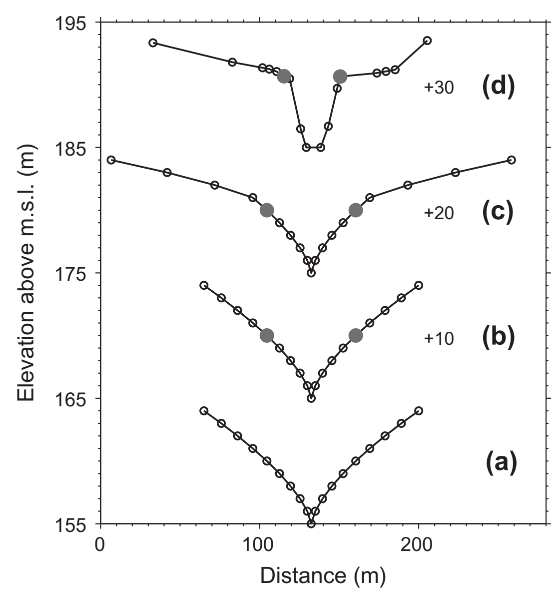

Fig. 3. Illustration of the different cross section parameterizations employed in the scenarios and baseline simulations. The cross sections are for a single location in the main stream reach of the Blue River basin. (a) Channel power law cross section shape with single roughness parameter, (b) channel power law cross section shape with different roughness parameter for the channel and floodplain sections (the gray dot indicates the separation between the channel and floodplain), (c) different power law cross section and roughness parameter for the channel and floodplain sections, and (d) detailed cross section data from field survey. The cross sections (b), (c), and (d) above have been offset by 10, 20, and 30, respectively, for clarity.

Fig. 3a illustrates the cross section shape used for the first scenario. This scenario is referred to as DW1. In DW1, we start with the same power law cross section shape and single roughness parameter used in the baseline HL-RDHM simulation (KW). Hence, the only difference with respect to KW is the use of dynamic wave routing, as opposed to the kinematic wave. The second scenario (referred to as DW2) uses the same shape as the previous scenario but changes the roughness value for the floodplain part of the cross section. We recognize that the previous is a simplified and often practical way of dealing with variability in the roughness value. However, a more general representation is possible for example as done in Orlandini (2002) and Camporese et al. (2010). Fig. 3b illustrates the cross section parameterization used in DW2. The third scenario (referred to as DW3) implements a power law floodplain shape and assumes different values for the channel and floodplain roughness. The cross section shape for this last scenario is illustrated in Fig. 3c. Table 2 summarizes the differences between the scenarios, including the two baseline simulations.

The three scenarios (DW1, DW2, and DW3) have in common the following characteristics: the only aspect of the coupled model changed in each scenario is the cross section parameterization (all other parameters and conditions remain the same), observed streamflows are used as the upstream boundary condition to emphasize changes along the portion of the main stream with detailed cross section data; dynamic wave routing is used in all the scenarios; the roughness parameters are re-calibrated for each scenario based on the approach of Section 3.2; and the analysis of results is focused on a selected set of individual storm events from the validation period.

5.2. Evaluation of simulations

For the evaluation of results, we select individual storm events to retain more information about the changes caused by each scenario. In total, we use 11 and 23 storm events for the Blue and Illinois River, respectively. The events are selected to represent different flow conditions (e.g. low and high flows), have different storm hydrograph duration, and come from different years. The lesser number of events selected for the Blue River is due to having a shorter record of observations and a considerably larger number of missing records. The events are all selected from the validation periods defined earlier in Section 3.3.

For the evaluation we employ the following four measures of performance and hydrograph agreement: NS, R_{mod}, $|\Delta Q_p|/Q_{p,obs}$, and $|\Delta T_p|/T_{p,obs}$. NS and R_{mod} were defined earlier. The measure $\Delta Q_p/Q_{p,obs}$ is the relative difference between the observed and simulated peak flow. $\Delta T_p/T_{p,obs}$ is the relative difference in the time to peak. The observed peak flow ($Q_{p,obs}$) and the observed time to peak ($T_{p,obs}$) are used as the normalizing quantities. ΔQ_p denotes the difference between the simulated and observed peak flow, and ΔT_p the difference between the simulated and observed time to peak. The measures $\Delta Q_p/Q_{p,obs}$ and $\Delta T_p/T_{p,obs}$ were chosen to allow consideration of multiple-criteria and because these measures are valued quantities in river forecasting (Fread, 1993). We will also use the percent difference in the average validation value of a measure between two simulations to quantify predictive gains or losses.

To further assess the degree of predictive changes and because NS values vary from storm to storm, we employ hypothesis testing (McCuen et al., 2006). Using hypothesis testing is analogous, in some respect, to the inclusion process followed in stepwise regression analysis to choose predictors. The objective is in this case to test, after a new cross section parameterization or scenario is tried, if changes caused in the value of NS by the new scenario can be considered statistically significant relative to a baseline scenario.

Specifically, the test is as follows (McCuen et al., 2006):

$$\begin{aligned} H_o &: NS_i = NS_{i,KW} \\ H_a &: NS_i > NS_{i,KW} \end{aligned} \tag{8}$$

where H_o and H_a are the null and alternative hypothesis, respectively. The subscript i indicates the test is applied to values obtained for the ith storm event. NS_i is the value from the current simulation, and $NS_{i,KW}$ is the value from the baseline HL-RDHM simulation (KW). The hypothesis tested in (8) is whether the NS value, for a given storm event i in the current simulation, can be considered the same or significantly different to the NS value from KW for event i. In (8), KW is used because this baseline simulation represents the model structure that we are seeking to improve. This evaluation strategy may be interpreted as reflecting a so-called top-down approach because the performance of the least detailed model structure is used to assess potential predictive gains from a more detailed one (Sivapalan et al., 2003). The test is only performed on NS values because NS and R_{mod} are related (McCuen et al., 2006). We selected a 10% level of significance for the hypothesis test. The exact definition of the test and critical statistic required by (8) are given in McCuen et al. (2006).

On the other hand, to ascertain if there is potential for achieving improvements from increasing the cross section complexity, we perform the following test (McCuen et al., 2006):

$$\begin{aligned} H_o &: NS_i = NS_{i,DW4} \\ H_a &: NS_i < NS_{i,DW4} \end{aligned} \tag{9}$$

The terms in (9) are the same as in (8), only the alternative hypothesis is changed. (9) may be representative of a so-called bottom-up approach in the sense that the most detailed model structure is used as reference (DW4) and compared against simulations with a simpler model structure (Sivapalan et al., 2003).

5.3. Comparison of baseline simulations

We compare first the baseline simulations (i.e. KW and DW4) to assess the ability of the coupled framework to improve predictions. Fig. 4 shows the values of these four evaluation measures for the baseline simulations and the selected storm events in the Blue River. In Fig. 4a and b, despite the observed variability, 8 out of 11 storm events have larger (better) NS and R_{mod} values, respectively, for the coupled baseline simulation.

The average values of the four measures shown in Fig. 4 are summarized in Table 1. The average values in Table 1 show that for the Blue River predictive improvement is possible when the

Table 2
Description of the different cross section parameterization scenarios, including the HL-RDHM (KW) and coupled (DW4) baseline simulations.

Simulation	Routing method	Cross section parameterization
KW[a]	Kinematic wave	Single power law cross section and single roughness coefficient
DW1	Dynamic wave	Single power law cross section and single roughness coefficient
DW2	Dynamic wave	Single power law cross section and different channel and floodplain roughness coefficient
DW3	Dynamic wave	Different power law cross section and roughness coefficient for channel and floodplain
DW4[b]	Dynamic wave	Detailed cross section with different roughness coefficient for channel and floodplain

[a] Baseline simulation obtained with HL-RDHM.
[b] Baseline simulation obtained by coupling HL-RDHM and HEC-RAS.

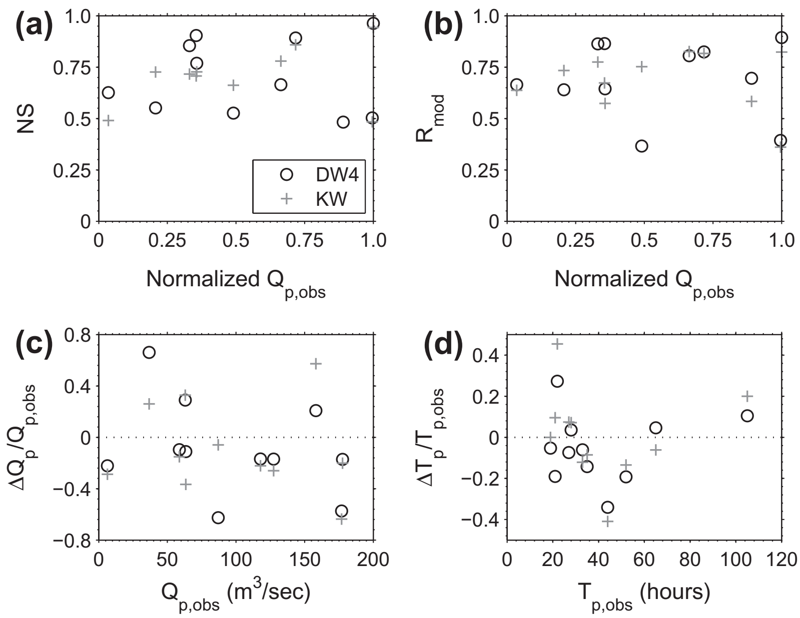

Fig. 4. Storm event values of (a) *NS*, (b) R_{mod}, (c) $\Delta Q_p/Q_{p,obs}$, and (d) $\Delta T_p/T_{p,obs}$ for the baseline simulations in the Blue River basin. The horizontal axis in (a) and (b) (normalized $Q_{p,obs}$) is estimated by dividing the value of the observed peak flow ($Q_{p,obs}$) for a given storm event by the maximum value of $Q_{p,obs}$ from all storm events. Each data point in the figures represents a different historical event simulation.

coupled baseline simulation (DW4) is compared against the HL-RDHM baseline simulation (KW). For example, the *NS* and R_{mod} increased by approximately 4% and 1.4%, respectively, while $|\Delta Q_p|/Q_{p,obs}$ and $|\Delta T_p|/T_{p,obs}$ decreased by roughly 1.3% and 11%, respectively, in DW4. Hence, for the Blue River, predictive gains are observed in the four measures with DW4.

Similarly for the Illinois River, when the two baseline simulations are compared, predictive gains are observed. For example, in Fig. 5a and b, this is apparent for the *NS* and R_{mod} values, respectively, associated with the storm events having the largest normalized $Q_{p,obs}$ value, say larger than about 0.75. These *NS* and R_{mod} values tend to be larger for DW4. Furthermore, looking at the average values in Table 1, from all the storm events considered in the Illinois River, we reach the same conclusion as in Blue based on 3 of the 4 measures. The average *NS* and R_{mod} values increase by approximately 3.5% and 1.2%, respectively, with DW4. While $|\Delta Q_p|/Q_{p,obs}$ actually increases by about 9.6% but $|\Delta T_p|/T_{p,obs}$ improves by 59%.

From applying the hypothesis test in (8) to the Blue and Illinois River, we found that 6 out of 11 and 17 out of 23 storm events, respectively, agree with the alternative hypothesis. Notice that the test in (8) is the same as the test in (9) for the baseline

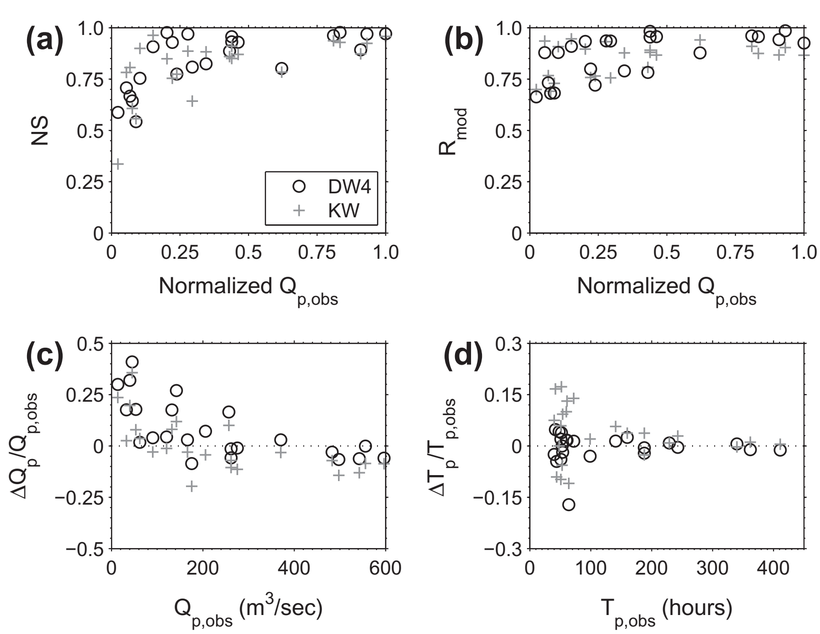

Fig. 5. Storm event values of (a) *NS*, (b) R_{mod}, (c) $\Delta Q_p/Q_{p,obs}$, and (d) $\Delta T_p/T_{p,obs}$ for the baseline simulations in the Illinois River basin. The horizontal axis in (a) and (b) (normalized $Q_{p,obs}$) is estimated by dividing the value of the observed peak flow ($Q_{p,obs}$) for a given storm event by the maximum value of $Q_{p,obs}$ from all storm events. Each data point in the figures represents a different historical event simulation.

simulations. In this case, the results of test (8) indicate that in more than half the events in the Blue and Illinois River, the *NS* value obtained for DW4 is significantly greater than the value for KW, suggesting further that in these two basins gains in predictive capability from the coupled framework are possible. Table 1 summarizes the results obtained for the hypothesis test in (8).

Importantly, the comparison just performed for the Blue and Illinois River, between the two baseline simulations, shows that the coupled framework is able to improve predictions. We will take in the next sections a more detailed view of this with the aim of understanding further the effects of cross section geometry complexity on simulation results. In doing so, we consider the statistical significance of these improvements, which appear relatively small based on average statistics (with the exception of the peak time improvement for the Illinois River). We also consider the magnitude of simulations improvements in the context of overall simulation uncertainty.

5.4. Effect of simplified routing

In this scenario (DW1) the goal is to assess the effects on predictions of simplified routing (i.e. from using kinematic instead of dynamic wave routing) assuming a power law cross section shape. By only looking at the model structure, the routing process in HL-RDHM can be thought to consist of two main simplifications: the kinematic wave approximation and the parameterized cross section shape (Koren et al., 2004). Both of these simplifications will cause some loss of predictive capability (Henderson, 1966; Fread, 1993; Butts et al., 2004). This first scenario will help distinguish the likely loss in predictive capability due to simplified routing.

For the simulation performed in this scenario, the average *NS* and R_{mod} validation values obtained for the Blue River are 0.7 and 0.69 (Table 1), respectively. The average values for the Illinois River are relatively greater ($NS = 0.84$ and $R_{mod} = 0.83$, Table 1). As expected from the lower average *NS* and R_{mod} values for the Blue River, its average $|\Delta Q_p|/Q_{p,obs}$ value is larger (0.32) than the average for the Illinois River (0.14). Similarly for $|\Delta T_p|/T_{p,obs}$, the Blue River has again a larger average value (0.15) than the Illinois River (0.081). This indicates that both the magnitude and timing of peak flows are in this case better estimated for storm events in the Illinois River than in the Blue River. Relative to the baseline HL-RDHM simulation (KW), the percent difference in the average *NS* validation values for the Blue River is 4.5% while there is no difference between the average R_{mod} values. Hence, in terms of R_{mod} alone, there are no gains from implementing dynamic wave routing in the Blue River, but the opposite is reflected in *NS*. For the Illinois River, the percent difference is 3.7% and −2.4% for *NS* and R_{mod}, respectively.

From applying the hypothesis test in (8) to the Blue and Illinois River, we found that 4 out of 11 and 9 out of 23 storm events (see Table 1), respectively, agree with the alternative hypothesis. Thus for the majority of events in the Blue and Illinois River, the differences in the value of *NS* between KW and DW1 can not be distinguished with respect to sampling variability, suggesting that in these two basins gains in predictive capability from dynamic wave routing alone may be somewhat unlikely.

For the Blue River, the test in (9) resulted in 3 out of 11 storm events with *NS* values less than NS_{DW4}, while in the Illinois River the result is 13 out of 23 (see Table 1). Based on this, it appears that further improvement may be realized for the Illinois River because there are many cases where the performance is less than DW4. In the Blue River the opposite seems the case, gains from a more detailed cross section shape may be unlikely. This is explored further in the next two scenarios.

5.5. Effect of the floodplain roughness parameter

To separate the effects of cross section geometry, and account for compensating effects in the roughness parameter (Horritt and Bates, 2002; Pappenberger et al., 2005), the only parametric change in this scenario (DW2) is the inclusion of a floodplain roughness parameter. The cross section shape is the same as in the previous scenario (DW1) and in the baseline HL-RDHM simulation (KW).

We found for this scenario that the average *NS* and R_{mod} value for the Blue River are improved, relative to the previous scenario, by 5.7% and 1.5%, respectively. The improvement is smaller for the Illinois River ($NS = 1.2\%$ and $R_{mod} = 0\%$). In terms of the average $|\Delta Q_p|/Q_{p,obs}$, and relative to the previous scenario, it decreases for the Blue River (−8.4%) and increases for the Illinois River (3.7%). The effects are reversed with respect to the average $|\Delta T_p|/T_{p,obs}$, it increases for the Blue River (11.3%) while it decreases for the Illinois River (−4.3%). Overall, based on these average values, gains in predictive capability from this scenario appear possible for both the Blue and Illinois River, further clarification is sought from tests (8) and (9).

For the test in (8), we found that in the Blue River 5 out of 11 events can be considered significant, while in the Illinois River 9 out of 23 events are significant. This indicates that for the Blue and Illinois River, even though some improvement is apparent on the average *NS* and R_{mod} values, the magnitude of the improvement is not as significant for the majority of events when accounting for the variability in *NS*. In other words, this suggests that the performance of this scenario is similar to the baseline HL-RDHM simulation for both basins. Further, the test in (9) indicates that 2 out of 11 and 13 out of 23 events in the Blue and Illinois River, respectively, are significantly less than DW4. Thus, further predictive gains may be possible in the Illinois River from a more detailed cross section shape but unlikely in the Blue River.

Thus far results from this and the previous scenario suggest that in the Blue River the kinematic wave approximation and the single power law cross section shape are only having a small impact on predictions since little improvement appears possible from including more cross section detail. The main reason for this, when contrasted against the Illinois River, appears to be the lower overall performance of the coupled model and the larger influence of lateral inflows in the Blue River. This results in greater uncertainty being propagated down the main stream reach (Carpenter and Georgakakos, 2006), and a diminished ability to produce gains through the routing process alone. More explanation on the hydrological modeling challenges and distinctive physical features involved in the simulation of flows in the Bluer River can be found in Koren et al. (2004), Smith et al. (2004a,b), and Carpenter and Georgakakos (2006).

5.6. Effect of the floodplain power law cross section shape

Although the influence of floodplains may be dependent on the flow magnitude, they can play an important role in flow routing (Horritt and Bates, 2002; Pappenberger et al., 2005; Nardi et al., 2006). This is typically recognized in hydraulic routing applications, e.g. flood mapping (Horritt and Bates, 2002; Pappenberger et al., 2005; Nardi et al., 2006). In hydrologic modeling the details about the floodplain cross section geometry are normally not considered (Koren et al., 2004; Carpenter and Georgakakos, 2006; Lian et al., 2007). Part of the reason for this may be the lack of cross section data and lack of simple empirical relationships for floodplain hydraulic geometry (e.g. Leopold–Maddock type relationships (Leopold and Maddock, 1953)). These limitations are becoming less of a constraint with the availability of high-resolution DEMs as well as recent findings in floodplain scaling (Dodov and Foufoula-Georgiou, 2005; Nardi et al., 2006). To provide supporting evidence for the implementation of the latter and assess further the required level of cross section detail, scenario DW3 is examined.

DW3 uses the channel and floodplain power laws in (2) and (7), respectively, and different roughness parameters for the channel and floodplain to define the cross section parameterization. The channel power law parameters are the same as in the previous scenarios (DW1 and DW2), the channel and floodplain roughness parameters are determined by re-calibration, and the floodplain power law parameters need to be estimated. To estimate the floodplain power law parameters, one of the approaches suggested by Fread and Lewis (1986) is followed. The value of the shape parameter d is selected first (see Eq. (7)) based on the available cross section data. For Blue we chose an expanding shape with $d = 1.6$. This is supported by the cross section data that shows a wide, and rather flat, floodplain for Blue. We chose $d = 0.2$ for Illinois also based on the available data which indicates a more parabolic shape. The parameter d is kept the same for all the cross sections while the parameter c (see Eq. (7)) is varied for each cross section. For both the Blue and Illinois River, the parameter c is estimated at each location in the main stream reach with a detailed cross section by selecting a few data points from the detailed cross section and then finding an average value of c in Eq. (7). Fig. 3c shows a representative cross section that combines a power law channel and floodplain cross section shape.

From the application of this scenario, we obtained an average NS and R_{mod} validation value equal to 0.7 and 0.69, respectively, for the Blue River, and 0.85 and 0.87, respectively, for the Illinois River (Table 1). As it was the case in the previous scenarios, the NS and R_{mod} gains in the Blue River are on the majority of cases not significant (5 out of 11 events for the test in (8)). For the Illinois River, relative to the previous scenario, there is a 4.8% gain in terms of R_{mod}. Improvement in Illinois is also reflected in the decrease caused by DW3 on the average values of $|\Delta Q_p|/Q_{p,obs}$ (−38.9%) and $|\Delta T_p|/T_{p,obs}$ (−33.9%).

Further, the test in (8) revealed that in the Illinois River 17 out of 23 events have NS values that are significantly greater than NS_{KW}, supporting the ability of the Illinois River to benefit considerably from this scenario. The test in (9) revealed that a lesser number of NS values can be considered to be less than NS_{DW1} (10 out of 23). The possibility of realizing predictive gains in the Illinois River from a more detailed cross section shape has been reduced, now the majority of events show insignificant gains, in contrast with the previous scenarios (DW1 and DW2) where gains were more likely. This may signify that for the Illinois River there is a limit in the gain of predictive capability possible from the coupled model structure, thereby suggesting that the simple power law floodplain shape is sufficient and the detailed cross section data may not be necessary. In fact, we arrive at the same conclusion when comparing the results from the test in (8) for this scenario and DW4. Both, DW3 and DW4, result in the same number of significant events.

6. Evaluation based on predictive uncertainty

As another way of evaluating the coupled simulations, predictive uncertainty is determined by estimating confidence intervals (CIs) using a stochastic method (Kelly and Krzysztofowicz, 1997; Montanari and Brath, 2004). The stochastic method employs a meta-Gaussian approach to estimate the probability distribution of the coupled model errors conditioned by the value of the simulated flows (Kelly and Krzysztofowicz, 1997; Montanari and Brath, 2004). This method is desirable because, within a spatially distributed and externally coupled framework, it is computationally efficient and straightforward to implement (Montanari and Brath, 2004).

To apply the meta-Gaussian model, it is assumed that the dependence of the normalized series of simulated flows and stabilized errors is linear and normal (Montanari and Brath, 2004). Ultimately the 90% CIs are estimated as follows (Montanari and Brath, 2004):

$$Q^{\pm}_{sim} = Q_{sim} + NQT^{-1}_{E'}[\mu(NE'(t)|NQ_{sim}) \pm 1.645\sigma(NE'(t)|NQ_{sim})]f(Q_{sim}) + \mu_{E'} \quad (10)$$

where Q^{+}_{sim} and Q^{-}_{sim} are the values of the upper and lower bounds, respectively. Q_{sim} is the simulated flow and E' denotes the stabilized errors. $NQT^{-1}_{E'}$ is the inverse of the standard normal quantile transform (maps the transformed errors back to non-normalized space). The NQT is also used to normalize the simulated flows (NQ_{sim}) and the stabilized errors ($NE'(t)$). $\mu(NE'(t)|NQt_{sim})$ and $\sigma(NE'(t)|NQ_{sim})$ are the conditional mean and standard deviation of the stabilized errors in normalized space, respectively. $f(Q_{sim})$ is the stabilizing function as proposed in Montanari and Brath (2004), and $\mu_{E'}$ is the mean of the stabilized errors. In (10), the ±sign is positive for the upper bound and negative for the lower bound. The details about the theory and derivations underlying the meta-Gaussian uncertainty method are reported elsewhere (Kelly and Krzysztofowicz, 1997; Montanari and Brath, 2004).

From (10) we determined the 90% CIs for the baseline coupled simulation (DW4). To evaluate the validity of the assumptions underlying the uncertainty method, the residuals from the linear regression of $NE'(t)$ on the series NQ_{sim} for DW4 are shown for the Blue and Illinois River in Figs. 6 and 7, respectively. Figs. 6a and 7a are used to verify the variance stabilizing transformation for the residuals while Figs. 6b and 7b verify the normality assumption. Both Figs. 6a and 7a do not show any marks of systematic deviations or a fan shaped residual cloud, suggesting that the errors are reasonably stable for both the Blue and Illinois River, respectively. Similarly, Figs. 6b and 7b show an acceptably good fit between the distribution of the residuals and the normal line for both the Blue and Illinois River, respectively, confirming they are approximately normal.

The application of (10) to represent CIs for the Blue River is illustrated in Fig. 8. Fig. 8 shows the 90% CIs for DW4 plotted with the hydrographs for all scenarios and baseline simulations, for six

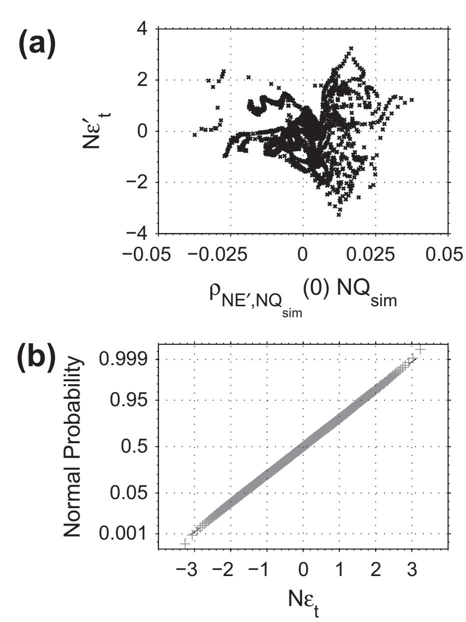

Fig. 6. Verification of the assumptions in the meta-Gaussian uncertainty method for the Blue River basin and the baseline coupled simulation. (a) Residual plot of the linear regression of $NE'(t)$ (stabilized errors) on the series NQ_{sim}. (b) Normal probability plot of the residuals of the regression of $NE'(t)$ on the series NQ_{sim}.

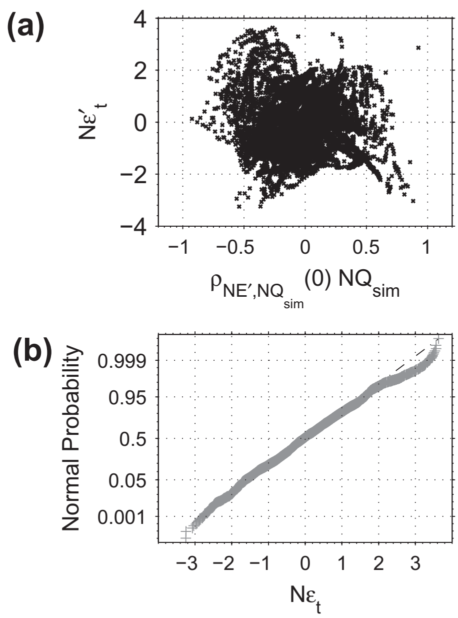

Fig. 7. Verification of the assumptions in the meta-Gaussian uncertainty method for the Illinois River basin and the baseline coupled simulation. (a) Residual plot of the linear regression of $NE'(t)$ (stabilized errors) on the series NQ_{sim}. (b) Normal probability plot of the residuals of the regression of $NE'(t)$ on the series NQ_{sim}.

individual storms events in the Blue River. From Fig. 8, the CIs for the Blue River tend to encompass the range of observations as well as the flows associated with the scenarios and baseline simulations. However, a tendency for the baseline HL-RDHM simulation to consistently have flows in the receding limb of the hydrographs that are outside the CIs is noted. This is possibly a benefit from implementing dynamic wave routing in the Blue River that could not be revealed by the performance criteria and hypothesis tests previously considered, but becomes apparent when the simulations and CIs are plotted in conjunction. To confirm that there is more of a dynamic effect in the Blue River, we examined the Froude number and the simulated stage-discharge rating curves from the HEC-RAS model for the Illinois and Blue River outlet points. For the Blue River, we found Froude numbers that are much less than 1 (approximately within the range 0.01-0.35) and observed that rating curves do exhibit more dynamic looping.

Fig. 9 shows the CIs and coupled simulations for six individual storm events in the Illinois River. As in the Blue River, the CIs tend to cover the range of flows associated with the observations, scenarios, and baseline simulations. However, the CIs are narrower in the Illinois River than in the Blue River. Take for example the event in Fig. 8d for the Blue River. For this event, the observed peak flow is approximately 180 m^3/s and the CIs about the observed peak range from approximately 60–200 m^3/s. A similar event in the Illinois River, say the event in Fig. 9b (which has a similar observed peak flow as the Blue River event in Fig. 8d), is bounded by CIs that are approximately equal to 120 and 190 m^3/s. This CI range is narrower (roughly half the size) than that in the Blue River. The estimated CIs are in general agreement with the results from Section 5, the relatively low performance of the Blue River simulations, as quantified for example by the NS coefficient, is associated with relatively larger predictive uncertainty, whereas in the Illinois River the opposite is observed.

Further, it seems likely that the coupled framework is able to reduce predictive uncertainty. Unfortunately, we can not compare the CIs for the two baseline simulations directly. We found in the

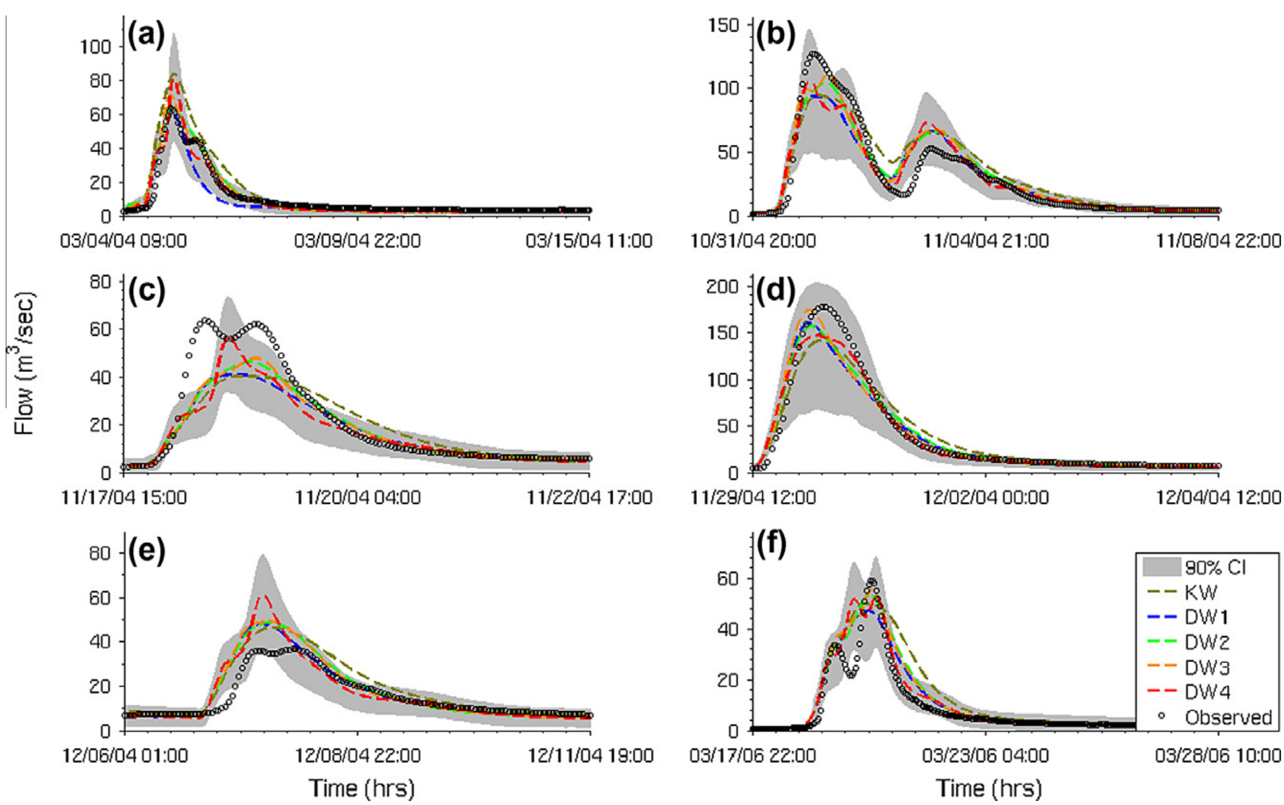

Fig. 8. Simulated flows and 90% CIs for six storm events in the Blue River basin during the validation period (observed streamflows at the upstream boundary). The simulated flows shown include the HL-RDHM baseline simulation (KW), the baseline coupled simulation (DW4), and the three cross section parameterization scenarios (DW1, DW2, and DW3). The 90% CIs shown are for DW4.

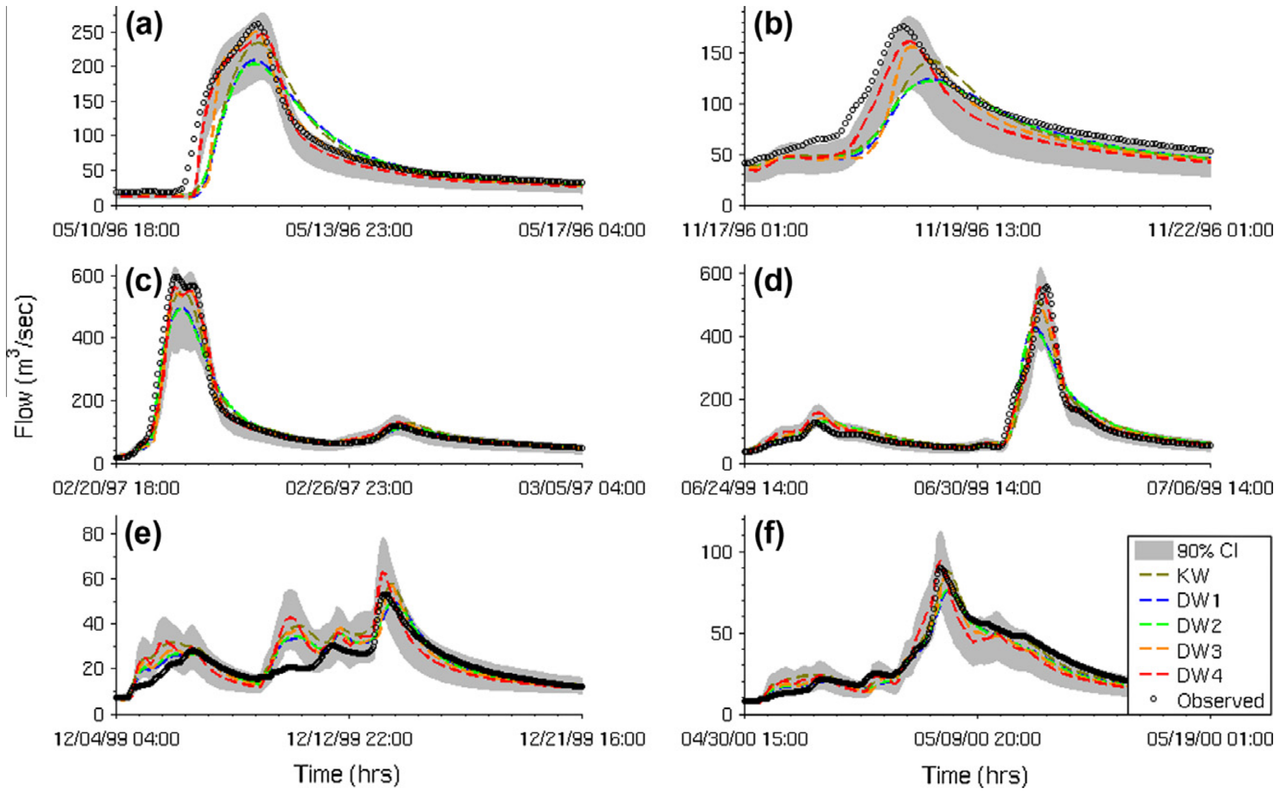

Fig. 9. Simulated flows and 90% CIs for six storm events in the Illinois River basin during the validation period (observed streamflows at the upstream boundary). The simulated flows shown include the HL-RDHM baseline simulation (KW), the baseline coupled simulation (DW4), and the three cross section parameterization scenarios (DW1, DW2, and DW3). The 90% CIs shown are for DW4.

CIs for KW important deviations from normality in its error distribution. However, as expected for a 90% level of confidence, approximately 10% of the observed data points for the baseline coupled simulation (DW4) fall outside the CIs. In contrast, for the baseline HL-RDHM simulation (KW), approximately 20% and 14% of the data fall outside the CIs for the Blue and Illinois River, respectively. In the Blue River, 5% and 15% of the data fall outside the lower and upper bound, respectively, and in the Illinois River 5% and 9%, respectively. This suggests that KW is likely to have a greater overall uncertainty than DW4 in both basins. Further, this observation follows from what we previously saw in the measures of model performance and the hypothesis tests on *NS* values for the baseline simulations. We saw that DW4 has a better performance, as reflected in the greater average *NS* and R_{mod} values, and that increases in the *NS* values tend to become more significant as one includes additional cross section detail and approaches the coupled baseline simulation, both of which imply less uncertainty in DW4.

7. Conclusions

From the application and evaluation of the coupled framework to the Blue and Illinois River basins, we can draw the following conclusions:

1. The comparison of the two baseline simulations indicated an ability to obtain predictive gains with the coupled framework. For example, in the Blue and Illinois River basins, the *NS* and R_{mod} improved with the coupling on average by approximately 3.9% and 1.3%, respectively. This type of coupled model structure, although somewhat more common for operational applications involving large rivers, is less common in hydrologic modeling of headwater basins, and its benefits in an operational modeling context are yet to be fully exploited.
2. For the first scenario tried, where the only change relative to the HL-RDHM baseline simulation was the use of dynamic wave as opposed to kinematic wave, we did not find a considerable improvement based on the evaluation performed. This we interpreted as indicating that dynamic wave alone may be unlikely to produce gains for flow predictions in the selected reach in the Blue and Illinois River basins.
3. The second scenario included an additional roughness parameter to differentiate between the conveyance of below and above bank-full flows. We found relative to the first scenario some improvement based on the *NS* and R_{mod} values. The values on average increased in both basins. However, from the hypothesis tests on *NS* values it was found that the improvements were not significant for the majority of the events. Based on the latter, we find little benefit in using an additional roughness parameter for the single power law cross sections in the Blue and Illinois River.
4. The last scenario, which considered different power laws for the channel and floodplain portions of the cross section, showed improvements in the Illinois River basin. These improvements were comparable to the ones obtained from using detailed cross section data. This suggests that detailed data may not always be necessary. This will need to be explored further and it could serve as a way to simplify data requirements in other applications of the coupled framework. This result is consistent with NWS dynamic hydraulic modeling experiences on large rivers where simplified cross section representations that preserve the approximate area-elevation relationships from detailed cross sections work well. Further, in terms of both the average *NS* and R_{mod} values, all the scenarios showed some improvement for Blue and only the last scenario showed improvements for Illinois.
5. The difficulties in achieving predictive gains for the Blue River from the scenarios tried are mostly attributed to the lower accuracy of runoff simulations and the larger contribution of

lateral inflows in this basin. The role played by these two factors could be another area for future work, as they could help define the conditions for which the coupled framework is most likely to produce benefits.

6. From the point of view of predictive uncertainty, there is a potential for decreasing overall uncertainty with the coupled framework. This we concluded from quantitative and qualitative assessments of the uncertainty associated with the baseline simulations, and by considering our previous findings based on measures of model performance and hypothesis testing. Additionally, the application of the stochastic uncertainty method demonstrated the usefulness of this method for estimating CIs when models are externally coupled.
7. Uncertainty analysis also visually highlighted limitations of the kinematic wave routing approach in matching the observed recessions for the Blue River, information that was not apparent through examination of measures of model performance alone. We hypothesize that this is due to dynamic loop effects in the Blue River. While this study evaluated model performance based on the ability to predict flow, future work on coupled frameworks of this type should also consider the ability to predict stage when dynamic loop effects are present.

To further apply this research to the distributed modeling efforts in OHD and fully exploit the benefits of the coupled framework, it is recommended that the coupling be enhanced so that information between the models can be transferred without manual intervention. This will not only facilitate implementation in an operational setting, but it will allow application to a larger number of basins, simultaneous hydrologic and hydraulic calibration, and uncertainty and/or sensitivity analysis. These in turn will help identify the largest sources of uncertainty and the role of lateral inflows and scale on coupled simulations. Additionally, to effectively use resources, it will be beneficial to develop a priori criteria for selecting those basins where the coupled framework is most likely to provide benefits.

Acknowledgements

This research was performed while the first author held a National Research Council Research Associateship Award at the Hydrology Lab of NOAA/NWS. We are thankful to the Editors, S. Orlandini, and an anonymous reviewer for their valuable comments, criticisms, and suggestions. They helped to improve the quality of the original manuscript. The authors also thank M. Smith and V. Koren of the Hydrology Lab for their helpful comments regarding this research.

References

Brunner, G.W., 2008a. HEC-RAS, River Analysis System Hydraulic Reference Manual. US Army Corps of Engineers. Hydrologic Engineering Center, Davis, 411pp.
Brunner, G.W., 2008b. HEC-RAS, River Analysis System User's Manual. US Army Corps of Engineers. Hydrologic Engineering Center, Davis, 733pp.
Butts, M.B., Payne, J.T., Kristensen, M., Madsen, H., 2004. An evaluation of the impact of model structure on hydrological modelling uncertainty for streamflow simulation. Journal of Hydrology 298 (1–4), 242–266.
Camporese, M., Paniconi, C., Putti, M., Orlandini, S., 2010. Surface-subsurface flow modeling with pathbased runoff routing, boundary condition-based coupling, and assimilation of multisource observation data. Water Resources Research 46 (2), W02512.
Carpenter, T.M., Georgakakos, K.P., 2006. Discretization scale dependencies of the ensemble flow range versus catchment area relationship in distributed hydrologic modeling. Journal of Hydrology 328 (1–2), 242–257.
Cook, A., Merwade, V., 2009. Effect of topographic data, geometric configuration and modeling approach on flood inundation mapping. Journal of Hydrology 377 (1–2), 131–142.
Dodov, B., Foufoula-Georgiou, E., 2005. Fluvial processes and streamflow variability: interplay in the scale-frequency continuum and implications for scaling. Water Resources Research 41, W05005.
Fread, D.L., 1981. In: Flood Routing: A Synopsis of Past, Present, and Future Capability, Proceedings, International Symposium on Rainfall–Runoff Modeling, Mississippi State University, Mississippi, pp. 521–541.
Fread, D.L., 1993. In: Maidment, D.R. (Ed.), Flow routing, in Handbook of Hydrology. McGraw-Hill, New York, pp. 10.1–10.36 (Chapter 10).
Fread, D.L., Lewis, J.M., 1986. In: Parameter Optimization for Dynamic Flood-Routing Applications with Minimal Cross-Sectional Data, Presented at and Published in the Proceedings of ASCE Water Forum '86 World Water Issues in Evolution, Long Beach, California.
Garbrecht, J., 1990. Analytical representation of cross-section hydraulic properties. Journal of Hydrology 119, 43–56.
Henderson, F.M., 1966. Open Channel Flow. Prentice Hall, New York, 522pp.
Horritt, M.S., Bates, P.D., 2002. Evaluation of 1D and 2D numerical models for predicting river flood inundation. Journal of Hydrology 268 (1–4), 87–99.
Keefer, T., 1976. Comparison of linear systems and finite difference flow-routing techniques. Water Resources Research 12 (5), 997–1006.
Kelly, K.S., Krzysztofowicz, R., 1997. A bivariate meta-Gaussian density for use in hydrology. Stochastic Hydrology and Hydraulics 11, 17–31.
Knight, D.W., 2006. River flood hydraulics: validation issues in one-dimensional flood routing models. In: Knight, D.W., Shamseldin, A.Y. (Eds.), River Basin Modelling for Flood Risk Mitigation. Taylor and Francis, Leiden, Netherlands, pp. 335–385 (Chapter 18).
Koren, V., Reed, S., Smith, M., Zhang, Z., Seo, D.-J., 2004. Hydrology laboratory research modeling system (HL-RMS) of the US national weather service. Journal of Hydrology 291 (3–4), 297–318.
Koren, V., Smith, M., Duan, Q., 2003. Use of a-priori parameter estimates in the derivation of spatially consistent parameter sets of rainfall–runoff models. In: Duan, Q., Gupta, H.V., Sorooshian, S., Rousseau, A.N., Turcotte, R. (Eds.), Calibration of Watershed Models, Water Science and Application, vol. 6. American Geophysical Union, Washington, DC, pp. 239–254.
Kuzmin, V., Seo, D.-J., Koren, V., 2008. Fast and efficient optimization of hydrologic model parameters using a priori estimates and stepwise line search. Journal of Hydrology 353 (1–2), 109–128.
Leopold, L.B., Maddock, T., 1953. The Hydraulic Geometry of Stream Channels and Some Physiographic Implications. US Geological Survey Prof. Paper 252, USGS, Washington, DC, 56pp.
Lian, Y., Chan, I-C., Singh, J., Demissie, M., Knapp, V., Xie, H., 2007. Coupling of hydrologic and hydraulic models for the Illinois River Basin. Journal of Hydrology 344 (3–4), 210–222.
Lin, Z., Beck, M.B., 2007. On the identification of model structure in hydrological and environmental systems. Water Resources Research 43, W02402.
McCuen, R., Knight, Z., Cutter, A.G., 2006. Evaluation of the Nash–Sutcliffe efficiency index. Journal of Hydrologic Engineering 11 (6), 597–602.
McCuen, R., Snyder, W., 1975. A proposed index for comparing hydrographs. Water Resources Research 11 (6), 1021–1024.
Myers, W.R.C., 1991. Influence of geometry on discharge capacity of open channels. Journal of Hydraulic Engineering 117 (5), 676–680.
Montanari, A., Brath, A., 2004. A stochastic approach for assessing the uncertainty of rainfall–runoff simulations. Water Resources Research 40, W01106.
Moreda, F., Gutierrez, A., Reed, S., Aschwanden, C., 2009. Transitioning NWS operational hydraulics models from FLDWAV to HEC-RAS. In: ASCE Conf. Proc. 342, 292, 11pp.
Nardi, F., Vivoni, E.R., Grimaldi, S., 2006. Investigating a floodplain scaling relation using a hydrogeomorphic delineation method. Water Resources Research 42, W09409.
Nash, J.E., Sutcliffe, J.V., 1970. River flow forecasting through conceptual models 1: a discussion of principles. Journal of Hydrology 10 (3), 282–290.
Pappenberger, F., Beven, K., Horritt, M., Blazkova, S., 2005. Uncertainty in the calibration of effective roughness parameters in HEC-RAS using inundation and downstream level observations. Journal of Hydrology 302 (1-4), 46–69.
Orlandini, S., Rosso, R., 1996. Diffusion wave modeling of distributed catchment dynamics. Journal of Hydrologic Engineering 1 (3), 103–113.
Orlandini, S., Rosso, R., 1998. Parameterization of stream channel geometry in the distributed modeling of catchment dynamics. Water Resources Research 34 (8), 1971–1985.
Orlandini, S., 2002. On the spatial variation of resistance to flow in upland channel networks. Water Resources Research 38 (10), 1197.
Ponce, V.M., Porras, P.J., 1995. Effect of cross-sectional shape on free-surface instability. Journal of Hydraulic Engineering 121 (4), 376–380.
Reed, S.M., 2003. Deriving flow directions for coarse-resolution (1–4 km) gridded hydrologic modeling. Water Resources Research 39 (9), 1238.
Reed, S., Koren, V., Smith, M., Zhang, Z., Moreda, F., Seo, D.-J., DMIP Participants, 2004. Overall distributed model intercomparison project results. Journal of Hydrology 298 (1–4), 27–60.
Reichert, P., Mieleitner, J., 2009. Analyzing input and structural uncertainty of nonlinear dynamic models with stochastic, time-dependent parameters. Water Resources Research 45, W10402.
Romanowicz, R., Beven, K.J., 2003. Estimation of flood inundation probabilities as conditioned on event inundation maps. Water Resources Research 39 (3), 1073.
Singh, V.P., 1996. Kinematic Wave Modeling in Water Resources, Surface-Water Hydrology. John Wiley & Sons, Inc., New York, 1424pp.
Singh, A.K., Porey, P.D., Raju, K.G.R., 1997. Criterion for location of downstream control for dynamic flood routing. Journal of Hydrology 196 (1–4), 66–75.
Sivapalan, M., Blöschl, G., Zhang, L., Vertessy, R., 2003. Downward approach to hydrological prediction. Hydrological Processes 17 (11), 2101–2111.

Smith, M.B., Koren, V., Zhang, Z., Cui, Z., 2009. Distributed hydrologic modeling: from research to operational forecasting. In: ASCE Conf. Proc. 342, 621.

Smith, M.B., Koren, V.I., Zhang, Z., Reed, S.M., Pan, J.-J., Moreda, F., 2004a. Runoff response to spatial variability in precipitation: an analysis of observed data. Journal of Hydrology 298 (1–4), 267–286.

Smith, M.B., Seo, D.-J., Koren, V.I., Reed, S.M., Zhang, Z., Duan, Q., Moreda, F., Cong, S., 2004b. The distributed model intercomparison project (DMIP): motivation and experiment design. Journal of Hydrology 298 (1–4), 4–26.

Valiani, A., Caleffi, V., 2009. Analytical findings for power law cross-sections: uniform flow depth. Advances in Water Resources 32 (9), 1404–1412.

Zhang, Z., Koren, V., Smith, M., Reed, S., Wang, D., 2004. Use of next generation weather radar data and basin disaggregation to improve continuous hydrograph simulations. Journal of Hydrologic Engineering 9 (103), 103–115.